Interfacing carbon nanotubes of arbitrary chiralities into linear heterojunctions

J. Bhattacharjee[1,2] and J. B. Neaton[1]

[1]*Molecular Foundry, Lawrence Berkeley National Laboratory, Berkeley, California 94720, USA*

[2]*National Institute of Science Education and Research, Bhubaneswar, Orissa, India*

(Received 17 September 2010; revised manuscript received 7 February 2011; published 21 April 2011)

Motivated by recent advances in synthesis and characterization of carbon nanotube (CNT) heterojunctions, we introduce a systematic approach for obtaining atomic geometries that connect two carbon nanotubes of different chiralities. Using our approach, it is straightforward to construct atomic interface geometries between two single-walled CNT's of arbitrary chiralities arranged at different orientations and angles. Our method generalizes existing approaches and is readily applicable to joining domains of graphene nanoribbons as well. As an example, we focus on linear heterojunctions, and we postulate the minimum number of simple topological defects required at the interface, and the preferred spatial arrangements, to obtain maximally linear heterojunctions given any two arbitrary chiralities. We also provide a physical picture of the defect structure of the resultant interface geometries using the results of classical force-field simulations.

DOI: 10.1103/PhysRevB.83.165432 PACS number(s): 81.07.Nb, 68.65.−k, 85.35.−p

I. INTRODUCTION

Since their discovery,[1] carbon nanotubes (CNT's) have long held great promise as central building blocks of mechanical and electrical components in a variety of nanoscale devices. Single-walled CNT's can be semiconducting or metallic, depending on their chirality (n,m), and usually maintain a single chirality over their entire length. However, it is also possible to grow or connect two CNT's of different chiralities, resulting in a zero-dimensional sp^2-bonded nanoscale interface, or heterojunction (HJ). Such CNT-HJ's themselves constitute a distinct subclass of carbon nanostructures, and could eventual play a role as active elements in all-carbon nanoelectronic devices.

Over 15 years ago, a theoretical study by Chico *et al.* predicted that a semiconducting-metallic CNT HJ would behave like a Schottky diode.[2] But because CNT HJ's occur rarely in nature, and because of the fundamental challenges associated with simultaneous structural characterization and electrical measurements at nanometer length scales, many properties of this important class of nanoscale interfaces have yet to be systematically studied. Novel transport behavior of semiconductor-metallic CNT HJ's has been reported, including rectification[3] and, more recently, molecular-scale quantum dot behavior[4] for a HJ of well-defined chiralities. Previous work on CNT-HJ's with scanning tunneling microscopy[5–7] revealed the presence of multiple interfacial pentagons and heptagons, which are the simplest topological defects possible in graphene without creating dangling bonds. While it is well known that a pair of such simple topological defects can be used to connect two CNT's[8,9] of different chiralities, previous theory has demonstrated that their electronic properties can depend critically on the number and arrangement of such defects.[2,10–12] The physical factors influencing the number of such defects and their spatial arrangement on formation—as well as how those structural properties are connected to potential device performance—are still largely unexplored.

CNT-HJ's are most often discovered by chance, primarily due to a dearth of controllable synthesis strategies. Yet recent advances in CNT-HJ synthesis may change this situation. For example, controlling the temperature during chemical vapor deposition[13] has been observed to alter chirality during growth. Direct fusing of two CNT's of dissimilar chiralities through current-induced annealing has also been recently reported.[14] Rayleigh scattering-based techniques[15] can be used to determine constituent chiralities, and when combined with precise electrical transport measurements through CNT-HJ's,[4] such studies would enable a systematic understanding of relationships between structure and electronic properties of single-walled CNT-HJ devices.

The advances in synthesis and characterization described above will lead to a need for additional atomistic theoretical work on this unique class of nanostructures. A central element of any atomistic theory of a CNT HJ device is an atomistic model of the interface. In principle, any two CNT's can be simply interfaced[8,9] using a single pentagon and a single heptagon. However, as discussed in Sec. II, to relieve strain such interfaces often result in HJ's *bent* at an appreciable angle. In contrast, CNT-HJ's reported in recent literature[4–6] are largely *linear*, suggesting that the interfacial atomic structure cannot be simply rationalized by one pentagon and heptagon.[8,9] In addition, existing schemes to connect dissimilar CNT's[8,9] cannot be extended to obtain coplanar connectivity between two dissimilar graphene domains.[16,17]

In this paper, we develop a general geometric approach for interfacing two single-walled CNT's of arbitrary chirality at arbitrary angles with a minimum number of topological defects. We illustrate our method by constructing HJ's between two CNT's that are linear in extent. Our approach constitutes a well-defined scheme for building atomic models of interfaces of connected CNT's or graphene nanoribbons[16,17] of arbitrary chirality, a useful starting point for future studies of the electronic and transport properties of carbon nanostructured materials.

In Sec. II, we start with the simplest approach to connect two single-walled CNT's with a single pentagon and heptagon, and illustrate how it often leads to bent HJ's. We then describe how the colinearity of the constituent CNT's increases systematically with the introduction of additional topological defects, and how a linear HJ emerges from an optimal minimum number of such defects. In Sec. III, we provide

examples connecting different types of CNT's, followed by a companion study of the effect of the arrangement of defects on the shape, i.e., relative orientation of the constituent CNT's of the HJ, and their energetics using an empirical force-field model. Although we focus on connecting CNT's of similar radii, our approach can be easily generalized to connect CNT's of different radii, as shown in Sec. II B, and also graphene nanoribbons. Based on the proposed scheme, freely available web-based software[18] has been made available to form linear HJ's from dissimilar CNT's of similar radii.

II. INTERFACING CARBON NANOTUBES

Upon unwinding, two single-walled CNT's of arbitrarily different chiralities (n,m) and (n',m') form graphene nanoribbons, with the graphene lattice in one ribbon rotated relative to that in the other by an angle that is not necessarily a multiple of 60°, as shown in Figs. 1(a) and 1(b). Thus the problem of connecting two CNT's can be reduced to that of connecting two graphene nanoribbons at different orientations. The chiralities of the two CNT's define two characteristic triangles ABC and $A'B'C'$ at the ends of the unwound ribbons, as shown in Fig. 1(b). To connect the two CNT's to form an (n,m)-(n',m') HJ, the irregular quadrangle $ABA'C$, formed by joining the two triangles by their circumferential sides BC and $B'C'$, as shown in Fig. 1(c), must be tiled with three-coordinated carbon atoms with minimally strained C-C bonds. Below we describe how this can be accomplished in a general way to achieve interfaces of increasing degree of linearity.

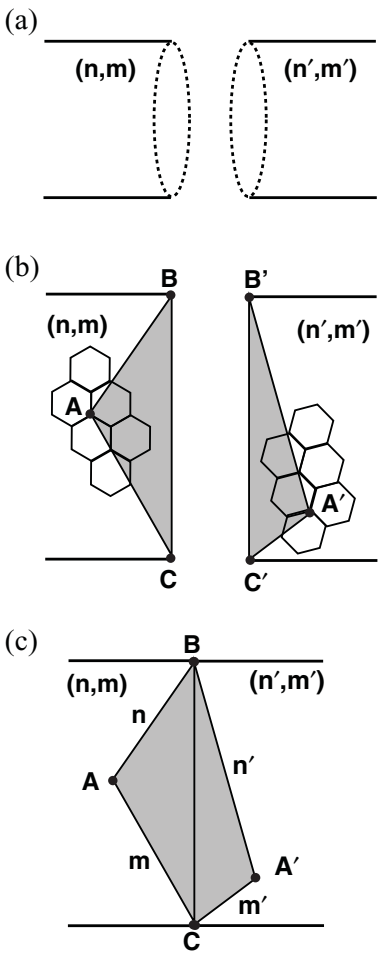

FIG. 1. (a) Two CNT's of similar radii but dissimilar chirality. (b) Characteristic triangles ABC and $A'B'C'$ at the edges of the two graphene ribbons due to unwinding of the CNT's. (c) Interface quadrangle $ABA'C$ formed by connecting the two characteristic triangles.

In what follows, minimum energy structures of CNT HJ's are obtained using Tersoff-Brenner[19,20] classical force fields. More specifically, we use a conjugate gradient minimization of the total energy $E_{\rm HJ}$, as computed with the empirical interatomic potential (EIP) introduced by Tersoff[19] and Brenner[20] (TB). This short-range and bond-order-type TB-EIP has been extensively used[21–23] in prior studies of carbon-based materials, including CNT's.

Based on the total energies of the optimized HJ's obtained using the TB-EIP force fields, we compute the strain energy associated with the interfaces connecting CNT segments of different chiralities. For all calculations, the HJ's are finite, consisting of two dissimilar finite CNT segments. The segments are chosen to be long enough so that in the middle of each segment, the effect of the uncapped ends is negligible, and the C-C bond lengths are converged to that for an infinite CNT of the same chirality. After optimizing the structure of an HJ, there are several C-C bonds in the vicinity of the interface, whose lengths depart from the respective bulk value. We refer to the energy associated with these strained bonds as the interfacial strain energy $E_{\rm strain}$. To calculate $E_{\rm strain}$ from the total energy $E_{\rm HJ}$, we first subtract out the total energy of a hypothetical HJ with the same C-C connectivity scheme but no strained C-C bonds. This gives us the total strain energy due to the interface and the two uncapped ends. Thus the strain energy of the interface, connecting two finite CNT segments 1 and 2, is given by

$$E_{\rm strain} = E_{\rm HJ} - N_{\rm HJ}E_0 - (E_{\rm end1} + E_{\rm end2}), \qquad (1)$$

where $N_{\rm HJ}$ is the total number of atoms in the HJ, and $E_{\rm end1(2)}$ is the strain energy associated with the uncapped end of tube 1 (2). Additionally, $E_0 = (E_1 + E_2)/2$, where E_1 (E_2) are the energy (atom) of periodic tubes of chiralities 1 and 2, with C-C bond lengths equal to their bulk value. The HJ's considered here are of length typically between 60 and 70 Å, with $N_{\rm HJ}$ in the range of 850–1050 atoms.

A. Illustrative example: Connecting (10-8)-(12,6) CNT's

To tile the "interface quadrangle" $ABA'C$ by three-coordinated atoms, the first task is to identify the smallest spatial region (or "patch") that cannot be tiled by hexagons alone. In Fig. 2(i)(a)–(c), we identify these patches as those without any solid C-C bonds within the context of a specific example, a (10,8)-(12,6) interface. The simplest way to "stitch up" the patch, particularly in the present case where $(n+m) = (n'+m')$, is to connect a pair of atoms sequentially as shown by dashed lines in Fig. 2(i)(a)–2(c). Straightforwardly, if $(n+m) \neq (n'+m')$, we need only to introduce extra "zigzag" ridges of number $|(n+m) - (n'+m')|$ within the patch. Note that in this simplistic approach to tiling the "patch," we would always obtain a single pentagon and a single heptagon, as shown with dark and light shading in Fig. 2(i)(a) .

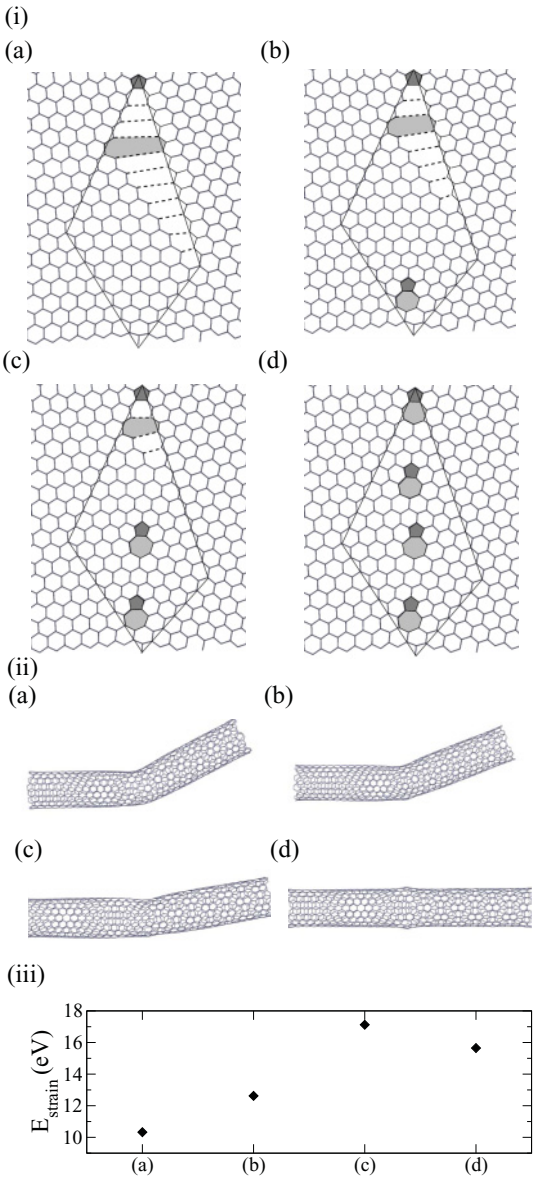

FIG. 2. (i)(a)–(d) Heterojunctions with different numbers of topological defects with CNT (10,8) on the left and CNT (12,6) on the right. (ii)(a)–(d) Corresponding energy-minimized structures. (iii) The net strain energies for the four different heterojunctions. For reference, within the empirical force-field model (TB-EIP) used in this work, the strain energy to create a single pentagon-heptagon paired defect in a CNT of similar radii is about 5.4 eV.

Thus the example shown in Fig. 2(i)(a) presents the simplest scheme to connect single-walled CNT's (10,8) on the left to (12,6) on the right. The C-C bonds indicated by dashed lines are under tensile strain, and each of the atoms would eventually need to relax further toward one other to form stable C-C bonds. As a result of the induced strain at the interface, the two graphene ribbons will no longer be coplanar; this implies that if the two ribbons are wound up, the two CNT's will not be collinear. In Fig. 2(ii)(a), we show the minimum energy structure of the HJ obtained with classical force fields.[19,20] This example indicates that to make the two CNT's maximally collinear, the simple solution is to reduce the number of unrealistically long C-C connectivities in the interface quadrangle, which is clearly beyond the scope of the simplest scheme involving a single pentagon and a single heptagon.

Figure 2(i)(b)–(d) illustrates that indeed, with the introduction of an increasing number of pentagon-heptagon (5-7) pairs, the number of unrealistically long C-C connectivities is reduced, reaching zero with the introduction of four such pairs of pentagons and heptagons. Concomitantly, the minimum energy structure of the HJ's becomes increasingly linear, i.e., the constituent CNT's become more collinear with the introduction of such defect pairs, as is evident from Fig. 2(ii)(b)–(d). Note that the HJ shown in Fig. 2(ii)(d) is perfectly linear, with only small protrusions and depressions localized at the 5-7 defect sites.

Strain energies corresponding to the four interfaces shown in Fig. 2(i)(a)–(d) are plotted in Fig. 2(iii). As is evident, the interface that results in a bent HJ [Fig. 2(ii)(a)] is least strained. This implies that the collinear structure of the (10,8)-(12,6) HJ with four 5-7 defects at the interface [Fig. 2(ii)(d)] is not thermodynamically favorable. However, to evolve into a less strained structure, the number of carbon atoms at the interface would have to be reduced, as the different connectivity schemes require different numbers of atoms to tile the interface quadrangle while preserving bond topology. This points to large activation barriers between the different HJ structures. Thus the collinear structure of the (10,8)-(12,6) HJ, which is not a global minima for strain energy, nevertheless can be locally stable under ambient conditions. However, as we show here, one can select chiralities of constituent CNT segments such that they form a thermodynamically favorable stable collinear HJ.

B. General approach for heterojunctions of increasing linearity

In the previous section, we have shown that introducing additional topological defects in a chirality-specific interfacial quadrangle can increase the linearity of CNT and GNR HJ's. In this section, we will outline an approach to determine the required type and number of topological defects to tile the interface quadrangle such that all the C-C bonds are minimally strained. This approach is general in that it can also be used to enumerate and position defects to interface CNT's at arbitrary angles.

To begin, we note that a single hexagon can be seen to constitute a "unit quadrangle" whose sides u,v,u',v'—which are similar to indices n,m,n',m' of the interface quadrangle—are all unity, as shown in Fig. 3(a). Therefore, if $n \neq m'$ and/or $n' \neq m$, the interface quadrangle cannot be tiled by

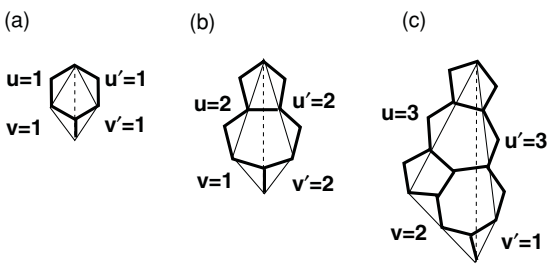

FIG. 3. The three basic quadrangles to be used as building blocks to tile the interface polygon.

hexagons alone; quadrangular building blocks of unequal sides are necessary. For example, to tile an interface quadrangle with $(n - m') = (n' - m) > 0$, similar quadrangular building blocks are required. The smallest block would have $(u - v') = (u' - v) = 1$. Specifically, $|n - m'|$ such building blocks, in addition to the unit quadrangles (i.e., simple hexagons), are needed to tile the interface quadrangle. Furthermore, if $(n - m') \neq (n' - m)$, similar quadrangular building blocks with $(u - v') \neq (u' - v)$ are needed to tile the interface quadrangle. The smallest such building block should therefore satisfy $(u - v') = 2, (u' - v) = 1$.

The smallest building block with $(u - v') = (u' - v) = 1$ is a 5-7 defect, a single pentagon and heptagon joined together through a common C-C bond, as shown in Fig. 3(b). We refer to this as a B-type building block. Similarly, the simplest quadrangular building block with $(u - v') = 2, (u' - v) = 1$ would be two 5-7 defects connected as shown in Fig. 3(c). We denote this structure as a C-type building block. This is demonstrated in Fig. 4, where the interface quadrangle shown in (a), connecting (7,5) and (6,6), has $(n - m') = (n' - m) = 1$, while the quadrangle shown in (b), connecting (8,5) and (6,6), has $(n - m') = 2, (n' - m) = 1$. Accordingly, the (7,5)-(6,6) and (8,5)-(6,6) HJ's require one B-type block and one C-type block, respectively, to complete the tiling of the interface quadrangle with three-coordinated carbon atoms. Note that the B- and C-type quadrangular blocks are shown as solid lines in Fig. 4, while the rest of the interface quadrangle can all be tiled with hexagons alone.

Having defined three irreducible quadrangular building blocks (Fig. 3)—a single hexagon (A) and two arrangements of 5-7 defects (B and C)—the next task is to determine the minimum number of B- and C-type blocks required to connect two CNT's of chiralities (n,m) and (n',m').

To simplify the following discussion, we assume $n \geqslant m', n' \geqslant m$, and $(n - m') \geqslant (n' - m)$, as shown in Fig. 1(c). The characteristic triangles of the two CNT's can always be oriented such that the resultant interface quadrangle satisfies these conditions. If p and q are the minimum numbers of B and C defect blocks inside the interface quadrangle, then its

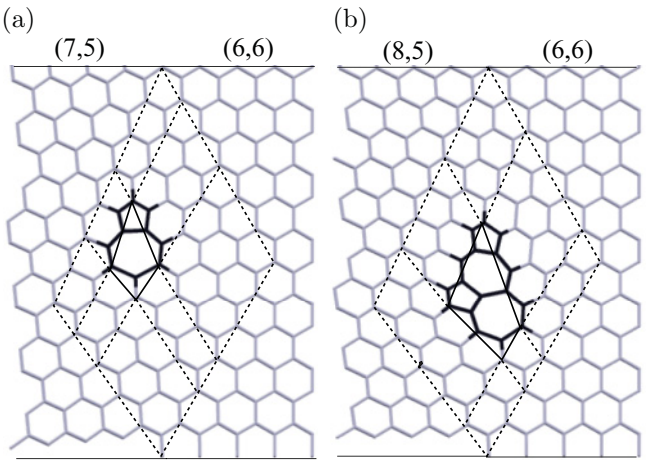

FIG. 4. HJ's made of CNT segments of chiralities (6,6) and (5,7) shown in (a) requiring one B-type block, and chiralities (6,6) and (5,8) shown in (b) requiring one C-type block, in order for the HJ's to be maximally linear.

opposing perimeter segments [(AB, CA') and (BA', AC) in Fig. 1] reduce in length by $(p + 2q)$ and $(p + q)$ in units of $|\vec{a}|$, with $\vec{a}$ being a primitive lattice vector of graphene. Thus,

$$n - m' = p + 2q, \tag{2}$$

$$n' - m = p + q, \tag{3}$$

which yield

$$p = 2(n' - m) - (n - m'), \tag{4}$$

$$q = (n - m') - (n' - m), \tag{5}$$

implying a total of $(n' - m)$ defect blocks.

It is important to note that there are two possibilities in which any two CNT's of dissimilar chirality can be connected. In one case, the n and m of one of the CNT's is reversed with respect to that in its counterpart in the other case. For example, as shown in Fig. 7(i)(a)–(h) and Fig. 8(i)(a)–(f), (10,8) and (12,6) CNT's can be interfaced to form linear (10,8)-(12,6) or (8,10)-(12,6) HJ's, with just two and four 5-7 defects, respectively. As shown in Sec. III, the HJ's with a higher number of 5-7 defects at the interface have a lower number of strained C-C bonds, and thus in general are more energetically favorable.

In the special case in which a HJ consists of $(n \neq 0, m \neq 0)$ and zigzag $(n',0)$ CNT's, the interface quadrangle reduces to a triangle. To connect two tubes in this case, one can convert the interface triangle to a quadrangle similar that of an $(n + 1,m)$-$(n',1)$ case. This is demonstrated in Fig. 5, which shows an interface triangle ABC connecting (8,10) to (16,0). The interface triangle ABC is expanded to the quadrangle $AB'C'C$, which connects (9,10) with (16,1). While rolling up ribbon, if we ensure that the segment AA' coincides with CC', then we effectively connect CNT (8,10) to CNT (16,0).

To join CNT's of different radii, building block C becomes more important. In fact, a single C block can, in principle, be thought to connect two CNT's of chiralities (3,2) and (3,1), whose radii, although unphysically small, are nevertheless substantially different. Accordingly, with three C blocks we can connect CNT's of chiralities $3 \times (3,2) \rightarrow (9,6)$ and $3 \times (3,1) \rightarrow (9,3)$, which are of radii 5.10 and 4.22 Å, respectively, as shown in Fig. 6(a). Figure 6(b) shows the energy-minimized structure of an HJ made of CNT's of chiralities (8,14) and (12,6) with radii 7.52 and 6.19 Å, respectively, through an interface quadrangle that incorporates four C-type blocks.

We note that the proposed scheme can be used to cap CNT's through a two-step process. First the CNT can be connected to an armchair $[(n,n)]$ edge of similar radius. Next the armchair edge can be capped using half of a fullerene of commensurate radius.

III. INTERFACIAL DEFECT ARRANGEMENT

Having established the minimal number of defects required to join two CNT's in a *collinear* fashion, we identify likely arrangements of defects within the quadrangle. To start, we consider the formation energetics of individual 5 and 7 defects. The obtuse interior angles between edges of pentagons (heptagons) are smaller (larger) than for regular hexagons. This results in compressive strain fields around pentagons and tensile strain fields around heptagons. For adjacent pentagons and heptagons, as in a 5-7 defect, these strain fields partially

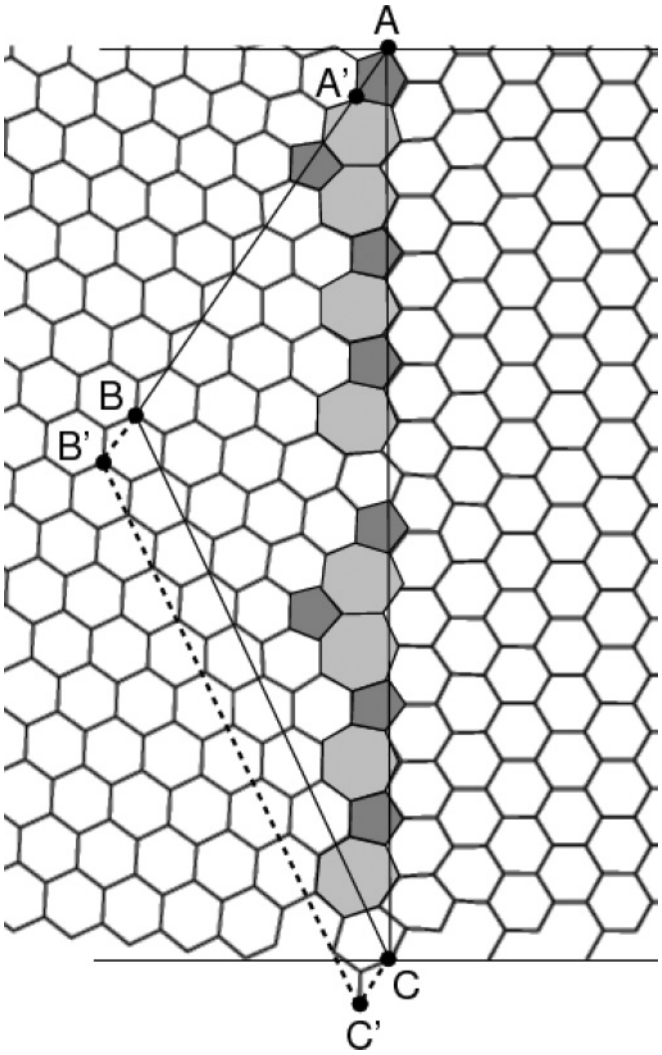

FIG. 5. Interface triangle ABC connecting CNT's (8,10) and (16,0).

compensate one another, reducing the total formation energy relative to isolated pentagons and heptagons. Further, when two 5-7 defects are in the vicinity of one another, arranged so that the pentagon of one is closer to the heptagon of the other, additional compensation of local strain fields will occur for similar reasons, reducing the overall strain energy, as in a Stone-Wales defect. Thus, we expect a tendency of defects at CNT HJ's to form in 5-7 pairs, and for these pairs to cluster in a manner that compensates their local strain fields.

To explore this more concretely, we focus on an (8,10)-(12,6) HJ, a system requiring only two B-type blocks

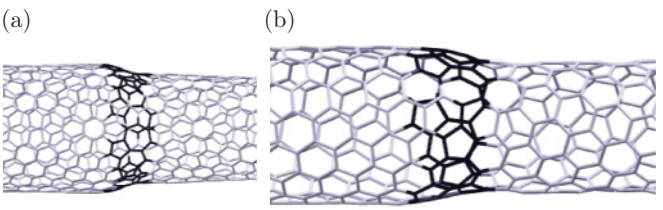

FIG. 6. (a) HJ composed of CNT's (9,6) and (9,3). (b) HJ composed of CNT's (14,8) and (12,6).

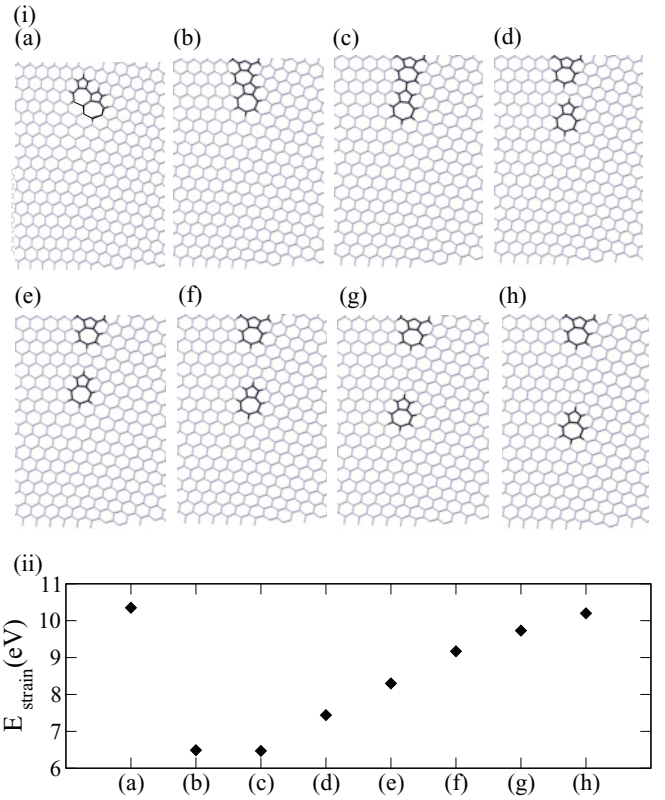

FIG. 7. (i)(a)–(h) Different arrangements of two defects at the interface of HJ (8,10)-(12,6). (ii)(a)–(h) Histogram plots of bond lengths in the corresponding energy-minimized structures. (iii) Net strain energies computed with TB-EIP.

(two 5-7 defects) to maintain connectivity within the interface quadrangle. Using force fields, we compute the local minima of energy for different separations between the two 5-7 defects along the circumference, as shown in Fig. 7(i)(a)–(h). In Fig. 7(ii), we plot strain energies as a function of separation for two 5-7 defects along the circumference. Interestingly, we find that a global minimum occurs when the two 5-7 defects are adjacent to each other, back-to-front, such that the heptagon of one of the 5-7 defects is adjacent to the pentagon of the other 5-7 defect, or at best separated by just one hexagon, as shown in Fig. 7(i)(b) and 7(i)(c). This sets the length scale for maximal cancellation of the strain fields of one 5-7 defect due to the other. The net strain increases with separation between two 5-7 defects oriented this way, as the mutual cancellation of strain fields diminishes. However, as argued earlier, there exist activation barriers between HJ's with different 5-7 arrangements, as the number of atoms required to tile the interface quadrangle varies systematically with defect separation. We expect the height of the activation barrier will be directly related to the degree of variation in the number of atoms tiling the interface quadrangle, which in general should increase as the number of 5-7 defects at the interface grows.

There are many ways to arrange B- and C-type blocks in the interface quadrangle. Different arrangements of four 5-7 defects at a (10,8)-(12,6) interface are shown in Fig. 8(i)(a)–(f). The corresponding energy-minimized structures shown in Fig. 8(ii)(a)–(f) suggest that linearity of the HJ increases with uniformity of distribution of the defects along the

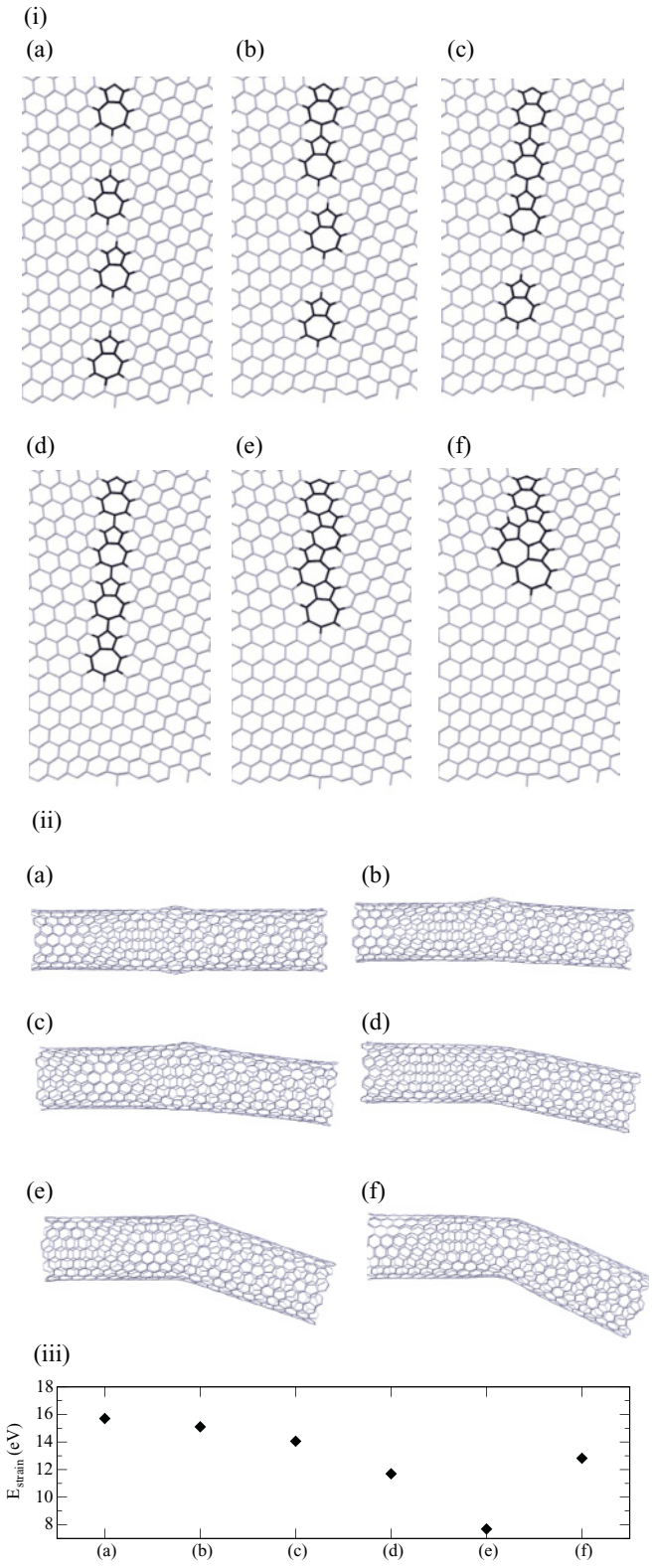

FIG. 8. (i)(a)–(f) Interface quadrangle showing different arrangements of the four 5-7 defects connecting CNT's (10,8) and (12,6). (ii)(a)–(f) Corresponding energy-minimized structures. (iii) Net strain energies computed with TB-EIP.

circumference. This arises from uniform mutual cancellation of strain due to the equispaced 5-7 defects. Net strain energies corresponding to different arrangements of four 5-7 defects are shown in Fig. 8(iii). A global minimum occurs when the four 5-7 defects are adjacent to each other back-to-front so that the heptagon of one defect sits next to the pentagon of the other, as shown in Fig. 8(i)(e). This is consistent with the global minimum found in the case of two adjacent 5-7 defects, and is consistent with 5-7 defects preferring to be adjacent to each other back-to-front, as shown in Fig. 7(i)(b).

The trends in the total energy and overall linearity of the HJ's as functions of the arrangement of defects suggest that in order for the linear HJ's to be energetically favorable, their interface defects must be sufficiently close to one another and be uniformly distributed around the circumference. This implies that, given any two CNT's, out of the two primary options for their connectivity—(m,n)-(m',n') and (n,m)-(m',n')—the one that requires the higher number of B and/or C blocks is a better candidate to form a linear HJ. Thus in reality there exist only a few chirality combinations that allow the formation of perfectly linear HJ's. We propose that if the chiralities of the two CNT's approximately satisfy the inequality

$$\mathrm{R} = \frac{\sqrt{m^2+n^2+mn} - (3q+2p)}{p+q} \leqslant 1, \tag{6}$$

then the HJ has a greater chance to be linear. The basis of the inequality is simply the assertion that defect blocks along the circumference should not be separated by more than one hexagon for linear HJ's to minimize strain energy. For (n,m) and (n',m') such that the defect blocks are separated by more than one hexagon, we expect that they may eventually migrate close to each other, which would then result in net unbalanced strain at the interface and consequently a bent HJ. Also, as the strain fields associated with the B- and C-type blocks differ in extent, for the linearity of an HJ, it is preferable that p and q are multiples of each other and both greater than 1. In the case of the HJ's studied here, the value of Re for the (10,8)-(12,6) HJ, with four 5-7 defects at the interface, is 1.9, while that for (8,10)-(12,6), with two 5-7 defects at the interface, is 5.8, implying that none of the HJ's are feasible candidates for a linear HJ. This is consistent with the optimized HJ's shown in Figs. 8 and 7, respectively. Instead, the (8,10)-(16,0) HJ, shown in Fig. 5, and with Re = 0.33, is expected to form a robust collinear HJ, as in this case defects can be uniformly arranged adjacent to each other back-to-front over the entire circumference.

IV. CONCLUSION

To conclude, we have discussed a class of single-walled CNT HJ's that are maximally linear in shape. We have shown the possibility of seamless collinear connectivity between two dissimilar CNT's through interfaces incorporating simple topological defects, whose type and numbers are unambiguously determined by the chiralities of the constituent CNT's. The same scheme can also be used to connect two graphene domains. We point out the criteria that the chiralities of the constituent CNT's should necessarily satisfy in order for the resultant linear HJ to be energetically favorable. With the advent of new experimental techniques[14] to controllably

make CNT HJ's, the structural algorithm proposed here can in principle guide the synthesis of linear HJ's for both fundamental studies and applications.

ACKNOWLEDGMENTS

J.B. thanks the National Institute for Science Education and Research (NISER) and the Department of Atomic Energy of the Government of India for generous support. Work at the Molecular Foundry was supported by the Office of Science, Office of Basic Energy Sciences, of the U.S. Department of Energy under Contract No. DE-AC02-05CH11231. Computational resources required for this work were partially provided by NERSC. We also acknowledge the National Science Foundation for support through the Network for Computational Nanotechnology (NCN).

[1] S. Ijima, Nature (London) **354**, 56 (1991).
[2] L. Chico, V. H. Crespi, L. X. Benedict, S. G. Louie, and M. L. Cohen, Phys. Rev. Lett. **76**, 971 (1996).
[3] Z. Yao, H. W. C. Postma, L. Balents, and C. Dekker, Nature (London) **402**, 273 (1999).
[4] B. Chandra, J. Bhattacharjee, M. Purewal, Y.-W. Son, Y. Wu, M. Huang, T. F. Heinz, P. Kim, J. B. Neaton, and J. Hone, Nano Lett. **9**, 1544 (2009).
[5] M. Ouyang, J.-L. Huang, C. L. Cheung, and C. M. Lieber, Science **291**, 97 (2001).
[6] M. Ouyang, J.-L. Huang, and C. M. Lieber, Acc. Chem. Res. **35**, 1018 (2002).
[7] H. Kim, J. Lee, S.-J. Kahng, Y.-W. Son, S. B. Lee, C.-K. Lee, J. Ihm, and Y. Kuk, Phys. Rev. Lett. **90**, 216107 (2003).
[8] B. I. Dunlap, Phys. Rev. B **49**, 5643 (1994).
[9] S. Melchor and J. A. Dobado, J. Chem. Inf. Comput. Sci. **44**, 1639 (2004).
[10] L. Chico, L. X. Benedict, S. G. Louie, and M. L. Cohen, Phys. Rev. B **54**, 2600 (1996).
[11] A. A. Farajian, K. Esfarjani, and Y. Kawazoe, Phys. Rev. Lett. **82**, 5084 (1999).
[12] M. Buongiorno Nardelli, Phys. Rev. B **60**, 7828 (1999).
[13] Y. Yao, Q. Li, J. Zhang, R. Liu, L. Jiao, Y. T. Zhu, and Z. Liu, Nat. Mater.**6**, 293 (2007).
[14] C. Jin, K. Suenaga, and S. Iijima, Nat. Nanotech. **3**, 17 (2008).
[15] M. Y. Sfeir, T. Beetz, F. Wang, L. M. Huang, X. M. H. Huang, M. Y. Huang, J. Hone, S. O'Brien, J. A. Misewich, T. F. Heinz, L. J. Wu, Y. M. Zhu, and L. E. Brus, Science **312**, (5773) 554 (2006).
[16] O. V. Yazyev and S. G. Louie, Phys. Rev. B **81**, 195420 (2010).
[17] O. V. Yazyev and S. G. Louie, Nat. Mater. **9**, 806 (2010).
[18] J. Ringgenberg, J. Bhattacharjee, J. B. Neaton, and J. C Grossman, doi:10254/nanohub-r4162.3 (2008).
[19] J. Tersoff, Phys. Rev. B **37**, 6991 (1988).
[20] D. W. Brenner, Phys. Rev. B **42**, 9458 (1990).
[21] S. Berber, Y.-K. Kwon, and D. Tománek, Phys. Rev. Lett. **84**, 4613 (2000).
[22] C. W. Padgett and D. W. Brenner, Nano Lett. **4**, 1051 (2004).
[23] D. Donadio and G. Galli, Phys. Rev. Lett. **99**, 255502 (2007).